AMERICAN SOCIETY FOR MICROBIOLOGY | Journal of Virology

Recapitulating Cross-Species Transmission of Simian Immunodeficiency Virus SIVcpz to Humans by Using Humanized BLT Mice

Zhe Yuan,[a] Guobin Kang,[a] Fangrui Ma,[a] Wuxun Lu,[a] Wenjin Fan,[a] Christine M. Fennessey,[b] Brandon F. Keele,[b] Qingsheng Li[a]

Nebraska Center for Virology, School of Biological Sciences, University of Nebraska—Lincoln, Lincoln, Nebraska, USA[a]; AIDS and Cancer Virus Program, Leidos Biomedical Research, Inc., Frederick National Laboratory for Cancer Research, Frederick, Maryland, USA[b]

ABSTRACT

The origins of human immunodeficiency virus type 1 (HIV-1) have been widely accepted to be the consequences of simian immunodeficiency viruses from wild chimpanzees (SIVcpz) crossing over to humans. However, there has not been any *in vivo* study of SIVcpz infection of humans. Also, it remains largely unknown why only specific SIVcpz strains have achieved cross-species transmission and what transmission risk might exist for those SIVcpz strains that have not been found to infect humans. Closing this knowledge gap is essential for better understanding cross-species transmission and predicting the likelihood of additional cross-species transmissions of SIV into humans. Here we show that humanized bone marrow, thymus, and liver (hu-BLT) mice are susceptible to all studied strains of SIVcpz, including the inferred ancestral viruses of pandemic and nonpandemic HIV-1 groups M (SIVcpzMB897) and N (SIVcpzEK505) as well as strains that have not been found in humans (SIVcpzMT145 and SIVcpzBF1167). Importantly, the ability of SIVcpz to cross the interspecies barrier to infect humanized mice correlates with their phylogenetic distance to pandemic HIV-1. We also identified mutations of SIVcpzMB897 (Env G411R and G413R) and SIVcpzBF1167 (Env H280Q and Q380R) at 14 weeks postinoculation. Together, our results have recapitulated the events of SIVcpz cross-species transmission to humans and identified mutations that occurred during the first 16 weeks of infection, providing *in vivo* experimental evidence that the origins of HIV-1 are the consequence of SIVcpz crossing over to humans. This study also revealed that SIVcpz viruses whose inferred descendants have not been found in humans still have the potential to cause an HIV-1-like zoonosis.

IMPORTANCE

It is believed that the origins of HIV-1 are the consequence of SIV from wild chimpanzees crossing over to humans. However, the origins of HIV-1 have been linked back to only specific SIVcpz strains. There have been no experiments that directly test the *in vivo* cross-species transmissibility of SIVcpz strains to humans. This is the first *in vivo* study of SIVcpz cross-species transmission. With the humanized-BLT mouse model, we have provided *in vivo* experimental evidence of multiple SIVcpz strains crossing over to humans and identified several important mutations of divergent SIVcpz strains after long-term replication in human cells. We also found that the cross-species transmission barrier of SIVcpz to humans correlates with their phylogenetic distance to pandemic HIV-1 group M. Importantly, this work provides evidence that SIVcpz viruses, whose inferred descendants have not been found in humans, still have the potential to cause a future HIV-1-like zoonotic outbreak.

Human immunodeficiency virus type 1 (HIV-1) infections have claimed millions of human lives since the pandemic began in 1981, and HIV-1 still infects about 2.3 million people every year (1, 2). Based on comparative phylogenetic analyses of HIV-1 and simian immunodeficiency viruses from chimpanzee (SIVcpz), it has been shown that AIDS is a zoonotic disease caused by cross-species transmissions of SIVcpz to humans (3, 4). HIV-1 is classified into M, N, O, and P groups, and each group is thought to have originated from an independent cross-species transmission. The HIV group M is the causative agent of pandemic HIV/AIDS; in contrast, group N, O, and P viruses infect only a limited number of individuals (5, 6). There are four subspecies of chimpanzees with distinct geographical distributions in Africa: *Pan troglodytes* subsp. *verus* in West Africa; *P. troglodytes* subsp. *vellerosus* in Nigeria and northern Cameroon; *P. troglodytes* subsp. *troglodytes* in southern Cameroon, Gabon, and the Republic of Congo; and *P. troglodytes* subsp. *schweinfurthii* in the Democratic Republic of Congo and countries to the East (7). The *P. troglodytes* subsp. *troglodytes* and *P. troglodytes* subsp. *schweinfurthii* chimpanzees harbor SIVcpz*Ptt* and SIVcpz*Pts*, respectively. It has been shown that specific lineages of SIVcpz from the wild chimpanzee *P. troglodytes* subsp. *troglodytes* in Africa have founded pandemic HIV-1 group M and nonpandemic group N infections; in contrast, SIVcpz in the wild chimpanzee *P. troglodytes* subsp. *schweinfurthii* or other strains from the *P. troglodytes troglodytes* group have not been found in humans (4–13). However, the reason for this difference is unknown and cannot be explained simply by geographical isolation, because SIVcpzMT145 also belongs to the *P. troglodytes troglodytes* group, but no human infection has been found.

It is impossible to conduct SIVcpz infection experiments in humans. Moreover, due to the lack of an *in vivo* experimental model, until now there has been no investigation of the initial interaction between SIVcpz and humans. Thus, some outstanding

Received 2 May 2016 **Accepted** 10 June 2016

Accepted manuscript posted online 15 June 2016

Citation Yuan Z, Kang G, Ma F, Lu W, Fan W, Fennessey CM, Keele BF, Li Q. 2016. Recapitulating cross-species transmission of simian immunodeficiency virus SIVcpz to humans by using humanized BLT mice. J Virol 90:7728–7739. doi:10.1128/JVI.00860-16.

Editor: Frank Kirchhoff, Ulm University Medical Center

Address correspondence to Qingsheng Li, qli@unl.edu.

questions remain. Can different SIVcpz strains readily infect humans? Why have only specific SIVcpz strains spilled over to humans? For those SIVcpz strains that have not been found in humans, do they still have the potential to cause an HIV-like zoonosis? How does SIVcpz adapt in the new human host? However, to date, there is no way to directly study the *in vivo* transmission of divergent strains of SIVcpz to humans.

The combination of human $CD34^+$ pluripotent hematopoietic stem cell transplantation with surgical engraftment of human fetal liver and thymic tissues results in improved immune cell reconstitution, maturation, and selection in humanized bone marrow, thymus, and liver (hu-BLT) mice. This hu-BLT mouse model is the best available animal model for humans (14, 15). Hence, hu-BLT mice provide an ideal *in vivo* model to test the infectivity of different strains of SIVcpz in humans and recapitulate the critical events of SIVcpz cross-species transmission to humans. In addition to the inferred ancestral viruses of HIV-1, chimpanzees or other nonhuman primates (NHPs) in Africa harbor other viruses that potentially can cause another pandemic zoonotic disease like HIV-1 in the future. Furthermore, there are more than 30 African NHP species that are infected with more than 40 different strains of simian immunodeficiency viruses (16). The conceptual framework and experimental system developed in this study can also be used to evaluate the potential risk of other emerging pathogens from nonhuman species, especially the great apes, to infect humans by cross-species transmission.

MATERIALS AND METHODS

Virus stock preparation. To generate virus, infectious molecular clones of SIVcpz (SIVcpzMB897, SIVcpzMB897-M30R, SIVcpzEK505, SIVcpzEK505-M30R, SIVcpzMT145, and SIVcpzBF1167) and HIV-1_{SUMA} were transfected into 293T cells. Briefly, 60 μg of plasmid DNA diluted into 120 μl Lipofectamine 2000 (Life Technologies) was used to transfect 293T cells. After 48 h of transfection, culture supernatant was collected and filtered through a 0.45-μm filter from each flask. A 35-ml volume of filtered medium was loaded into each Ultra-Clear tube (Beckman Coulter) for ultracentrifugation. Virus ultracentrifugation was conducted with an Optima L-100X ultracentrifuge and an SW 32 Ti rotor (Beckman Coulter) at 25,000 rpm for 90 min at 4°C. Supernatant was discarded, and the pellet was resuspended into 1 ml fresh medium, aliquoted into 200 μl in each sterile screw-cap vial, and stored at −150°C. Virus stocks were titrated on the TZM-bl reporter cell line with an X-Gal (5-bromo-4-chloro-3-indolyl-β-D-galactopyranoside) staining kit (Genlantis). Titers are expressed as TZM-bl infectious units (IU) per ml.

Generation of hu-BLT mice. Hu-BLT mouse generation and assessment of human immune cell reconstitution were conducted as we previously reported (17, 18) at the University of Nebraska—Lincoln Life Sciences Annex in accordance with Institutional Animal Care and Research Committee-approved protocols. Briefly, 6- to 8-week-old female NSG mice (NOD.Cg-Prkdcscid Il2rgtm1Wjl/SzJ, catalog number 005557; Jackson Laboratory) were housed and maintained in individual microisolator cages in a rack system capable of managing air exchange with prefilters and HEPA filters (0.22 μm). Room temperature, humidity, and pressure were controlled, and air was also filtered. On the day of surgery, mice received whole-body irradiation at the dose of 12 cGy/gram of body weight with the RS200 X-ray irradiator (RAD Source Technologies, Inc., GA) and were then implanted with one piece of thymic tissue fragment sandwiched with two pieces of human fetal liver tissue fragments under the murine left renal capsule. Within 6 h of surgery, mice were injected via the tail vein with 1.5×10^5 to 5×10^5 $CD34^+$ hematopoietic stem cells isolated from human fetal liver tissues. Human fetal liver and thymus tissues were procured from Advanced Bioscience Resources (Alameda, CA). After 9 to 12 weeks, human immune cell reconstitution in peripheral blood was measured by a fluorescence-activated cell sorter (FACS) Aria II flow cytometer (BD Biosciences, San Jose, CA) using antibodies against mCD45-APC, hCD45-FITC, hCD3-PE, hCD19-PE/Cy5, hCD4-Alexa 700, and hCD8-APC-Cy7 (catalog numbers 103111, 304006, 300408, 302209, 300526, and 301016, respectively; BioLegend, San Diego, CA). Raw data were analyzed with FlowJo (version 10.0; FlowJo LLC, Ashland, OR). All mice used in this study had high human immune reconstitutions with a ratio of $hCD45^+$ cells to a combination of $hC45^+$ cells and $mCD45^+$ cells in peripheral blood higher than 50%. The mice were randomly assigned into experimental groups with similar immune reconstitution levels (Table 1).

High-dose SIVcpz infections of hu-BLT mice. To test human susceptibility to SIVcpz, 25 female hu-BLT mice with high immune reconstitution were randomly divided into 5 groups (Table 1), and each mouse was inoculated intraperitoneally (i.p.) with a high dose ($3 \times 10^4 \pm 0.2 \times 10^4$ IU) of SIVcpzMB897, SIVcpzEK505, SIVcpzMT145, SIVcpzBF1167, or HIV-1_{SUMA}, respectively. Peripheral blood was collected weekly in the first 4 weeks postinoculation (wpi) and once every 2 weeks thereafter. At 16 wpi, mice were euthanized and the tissues of spleen, lymph node, kidney lymphoid organoid, and jejunum were collected and fixed in 4% paraformaldehyde (PFA) and SafeFix II (Fisher Scientific) for *in situ* tissue analyses. A few hu-BLT mice developed graft-versus-host disease before 16 weeks and were sacrificed for humane reasons. Fresh tissue was immediately frozen into liquid nitrogen for RNA extraction.

Cross-species transmission barrier of SIVcpz. To quantify the cross-species transmission barrier of SIVcpz to infect humans, each of the SIVcpz strains and HIV-1_{SUMA} was titrated based on viral reverse transcriptase (RT) activity, which is the best available method (19). The RT was measured in triplicate using the EnzChek reverse transcriptase assay kit (Invitrogen, Eugene, OR, USA). The virus strains were lysed using 10% Triton X-100 (final concentration, 1%) in RPMI medium supplemented with 10% fetal bovine serum (FBS), and HIV-1 reverse transcriptase (CHIMERx, Milwaukee, WI, USA) was used for the standard curve. Hu-BLT mice with good immune reconstitution were divided into 5 groups ($n = 6$ for SIVcpzMB897, and $n = 5$ for other strains), from which each mouse was inoculated i.p. with a low dose (0.52 U/mouse) of SIVcpz or HIV-1_{SUMA}, respectively (Table 1). At 2 and 4 wpi, pVL was measured to determine infection status. If pVL was negative at 4 wpi, the animal was considered uninfected and would receive another round of virus inoculation and pVL measurement at 2 and 4 wpi, until all the animals were infected. To determine the interspecies barrier, the Kaplan-Meier plot for conversion to infected status for each SIVcpz group was compared to that of HIV-1_{SUMA}, and Kaplan-Meier plots for conversion to infected status between different SIVcpz strain groups were also compared.

Competition of wild-type SIVcpz versus the Gag M30R mutant. To compare the *in vivo* fitness of wild-type SIVcpz and its Gag M30R mutant counterpart, hu-BLT mice ($n = 6$/group) were inoculated with a 1:1 mix of wild-type SIVcpzMB897 or SIVcpzEK505 with its Gag M30R mutant counterpart, respectively. We used inoculum containing both equal copy numbers of wild-type and mutant mix ($n = 3$) or equal infectious units of wild-type and mutant mix ($n = 3$), since the latter would eliminate the possibility that an equal-copy-number inoculum may contain an unequal number of infectious viruses. The doses of equal-copy-number mix for each wild-type and mutant were 1.53×10^9 for SIVcpzMB897 and 4.1×10^8 for SIVcpzEK505 copies/mouse, respectively; and the doses of equal infectious unit mix for SIVcpzMB897and SIVcpzEK505 were 1.5×10^4 and 1.4×10^4 IU/mouse, respectively (Table 1). At 4 wpi, the mice were euthanized and full-length *gag* sequences from plasma were amplified and sequenced using Sanger's method.

pVL. Plasma viral RNA (vRNA) was extracted using a QIAamp Viral RNA minikit (Qiagen). Plasma viral load (pVL) was conducted using reverse transcriptase quantitative PCR (qRT-PCR) on a C1000 Thermal Cycler and the CFX96 Real-Time system (Bio-Rad) and the TaqMan Fast Virus 1-Step master mix (Life Technologies). SIVcpz strain-specific primers and probes (Table 2) were designed, and no crossover signal was found

TABLE 1 Profiles of hu-BLT mice used in the experiments

Study, expt group ID, and animal ID	$hCD45^+$ cells/($hCD45^+$ + $mCD45^+$ cells) (%)	% of $hCD3^+$ in $hCD45^+$ cells	% of $hCD8^+$ in $hCD45^+$ $hCD3^+$ cells	% of $hCD4^+$ in $hCD45^+$ $hCD3^+$ cells
High-dose virus infectivity study				
MB897				
272[a]	67.60	82.60	16.40	80.90
273[a]	71.70	73.80	17.30	80.40
299	58.00	48.10	35.80	62.80
308[a]	63.50	40.40	22.20	73.50
316	57.20	30.50	37.70	56.30
EK505				
281	85.80	45.10	14.30	82.60
300[a]	58.80	52.20	20.30	76.30
310	65.50	23.40	28.70	64.80
312[a]	57.30	25.00	35.10	58.60
314[a]	86.80	8.67	37.90	42.20
MT145				
321[a]	87.30	66.80	12.90	83.40
331	62.60	68.40	12.50	83.90
336[a]	68.40	50.70	13.50	82.40
337	78.40	54.40	14.40	82.30
339[a]	64.70	70.00	13.60	81.70
BF1167				
480[a]	85.90	49.00	16.40	82.00
481	89.20	54.80	15.50	82.70
482[a]	80.10	64.40	11.00	85.20
483[a]	88.50	57.70	12.80	84.60
484	84.40	44.70	18.60	79.80
SUMA				
564	91.70	37.10	21.00	75.70
565	86.30	46.80	13.90	84.00
567	94.30	69.70	14.60	83.30
569	91.60	36.20	14.80	82.40
570	93.50	33.30	21.30	75.90
Low-dose cross-species transmission barrier study				
SUMA				
585	94.40	6.84	39.30	55.50
587	81.20	30.00	29.90	65.10
588	92.80	62.90	19.50	77.60
592	76.80	35.00	28.80	68.60
593	89.10	49.60	20.30	77.30
Avg	86.86	36.87	27.56	68.82
MB897				
566	80.20	29.40	28.00	69.00
578	87.90	32.40	19.90	76.80
584	87.40	9.81	48.40	48.20
590	84.40	49.20	17.20	80.00
613	80.80	86.90	10.40	88.80
619	82.60	66.90	11.10	88.10
Avg	83.88	45.77	22.50	75.15
EK505				
581	88.70	11.50	36.10	58.90
586	82.40	85.10	13.40	84.90
589	89.80	28.30	23.30	72.50
591	94.80	48.80	23.00	73.50
597	75.80	38.60	15.50	81.20
Avg	86.30	42.46	22.26	74.20

(Continued on following page)

TABLE 1 (Continued)

Study, expt group ID, and animal ID	hCD45$^+$ cells/(hCD45$^+$ + mCD45$^+$ cells) (%)	% of hCD3$^+$ in hCD45$^+$ cells	% of hCD8$^+$ in hCD45$^+$ hCD3$^+$ cells	% of hCD4$^+$ in hCD45$^+$ hCD3$^+$ cells
MT145				
530	54.40	36.20	20.20	76.50
562	79.80	12.90	26.00	69.50
568	95.80	54.00	13.20	83.20
574	95.00	47.30	21.60	74.40
596	82.30	26.80	24.60	72.50
Avg	81.46	35.44	21.12	75.22
BF1167				
575	90.60	26.40	18.60	77.70
594	78.90	50.50	28.30	68.90
595	88.00	32.30	15.30	82.40
598	93.50	45.50	19.40	77.50
599	79.80	13.10	53.00	41.80
Avg	86.16	33.56	26.92	69.66
M30R *in vivo* competition study				
MB897				
494	81.10	27.40	12.50	85.00
492	87.30	42.70	17.00	78.50
501	86.70	56.80	13.20	84.30
488	81.20	32.60	14.70	82.90
487	87.50	45.80	15.60	80.80
503	91.80	58.30	12.70	84.30
Avg	85.93	43.93	14.28	82.63
EK505				
486	94.30	42.50	12.00	85.30
496	90.80	58.90	10.70	87.50
500	90.40	21.90	22.50	73.20
490	87.30	31.20	10.90	86.30
491	86.00	33.60	11.90	85.80
504	86.10	62.70	11.10	87.30
Avg	89.15	41.80	13.18	84.23

[a] Viral genes for this animal have been sequenced.

among different strains. The detection limit of pVL was 200 copies/ml, which was determined through repeating endpoint detection of serial dilution of the AcroMetrix HIV-1 Panel (Life Technologies).

ISH and IHC staining. Viral RNAs in tissues were detected using *in situ* hybridization (ISH) by following our previously reported protocol (20). To generate sense and antisense SIVcpz strain-specific probes, the full-length *gag* and *env* genes of SIVcpz were amplified using RT-PCR with strain-specific primers (Table 2). The amplicons were cloned into the pCR4 Blunt-TOPO vector (Thermo Fisher Scientific). Insert orientation was determined by sequencing with T3 and T7 primers at Sequetech (Mountain View, CA), and plasmid DNA was linearized with restriction enzyme NotI or Pme I (New England BioLabs), from which ^{35}S-labeled antisense and sense probes were synthesized *in vitro*. Sense probe was used as negative control. After 14 days of exposure, in the developed radioautographs viewed with transmitted light, the vRNA$^+$ cells appear as black dots; viewed with epipolarized light, the vRNA$^+$ cells appear as blueish or greenish dots because of the large numbers of silver grains overlying the cell. To define the SIVcpz-infected cell type, the combined ISH and immunohistochemical (IHC) staining was conducted as previously reported (20). Overnight exposure was used. Anti-CD4 rabbit monoclonal antibody (EPR6855, 1:100 dilution; Abcam) and a cocktail of mouse monoclonal anti-CD68 (KP1, 1:100 dilution; Leica), anti-Ham56 (HAM56, 1:100 dilution; Dako), and anti-CD163 (10D6, 1:100; Leica) antibodies were used to identify CD4$^+$ T cells and macrophages, respectively. We manually counted about 200 viral RNA$^+$ cells to determine the percentage of colocalization of viral RNA with CD4$^+$ T cells or macrophages.

Sequencing of viral genes. To assess the *in vivo* adaptions of SIVcpz, vRNA was extracted from plasma with the RNeasy Plus minikit (Qiagen) from SIVcpzMB897- and SIVcpzBF1167-infected hu-BLT mice at 14 wpi (n = 2 and 3, respectively). The cDNA was synthesized using a strain-specific primer (Table 2) and Superscript III reverse transcriptase (Life Technologies). The cDNAs were amplified using Q5 Hot Start High-Fidelity DNA Polymerase (New England BioLabs) with strain- and gene-specific primers (Table 2). The amplicons were confirmed by 1.0% agarose gel stained with ethidium bromide, and bands were cut and purified by using the GeneJET gel extraction kit (Thermo Scientific). The amplicons of full-length *gag*, *pol*, and *env* regions for each sample were directly sequenced using Sanger's method at Sequetech (Mountain View, CA) or by next-generation sequencing (NGS; Illumina Genome Analyzer IIx) at the University of Nebraska Genomics Core (Lincoln, NE). PCR amplicons of some genes were also cloned into the pCR4 Blunt-TOPO vector (Thermo Fisher Scientific) for cloning sequencing at Sequetech (Mountain View, CA). Sequencing primers were designed based on primer walking. The sequences were manually examined peak by peak and assembled individually using Sequencher 5.0 (Gene Codes CorP., Ann Arbor, MI) after the ends of sequences containing ambiguous nucleotides were trimmed. The sequences were confirmed by overlapping identical regions. All the data obtained by bulk, cloning, and next-generation sequencing were analyzed and compared.

Bioinformatics analysis. The phylogenetic tree showing the evolutionary relationship between strains of SIVcpz and HIV-1 in Fig. 1 was made from *pol* sequences of SIVcpz, SIVgor, and HIV-1 groups M, N, O,

TABLE 2 Primers and probes used in this study

Assay and virus strain	Sequence[a]
Plasma viral load expt	
SIVcpzMB897	F: GCCTCAATAAAGCTTGCCTGAG
	R: GGGCGCCACTGCTAGAGA
	P: /56-FAM/CCAGAGTCA/ZEN/CAAATTGGATGGGCACA/3IABkFQ/
SIVcpzEK505	F: GCCTCAATAAAGCTTGCCTTGA
	R: GGGCGCCACTGCTAGAGA
	P: /56-FAM/CCAGAGTTA/ZEN/CCGAATGGATGGGCACA/3IABkFQ/
SIVcpzMT145	F: GCCTCAATAAAGCTTGCCTTGA
	R: GGGCGCCACTGCTAGAGA
	P: /56-FAM/CCAGAGTCA/ZEN/CTGAATAGACGGGCACA/3IABkFQ/
SIVcpzBF1167	F: CGCTCAATAAAGCTTGCCTGAG
	R: GGGCGCCACTGGTAGAGA
	P: /56-FAM/GCGGAATGA/ZEN/GATGGGCACACACTGAT/3IABkFQ/
HIV-1	F: GCCTCAATAAAGCTTGCCTTGA
	R: GGGCGCCACTGCTAGAGA
	P: /56-FAM/CCAGAGTCA/ZEN/CACAACAGACGGGCACA/3IABkFQ/
RT primers	
SIVcpzMB897	AGGCAAGCTTTATTGAGGCTTAAGCAG
SIVcpzEK505	AGGCAAGCTTTATTGAGGCTTAAGCAG
SIVcpzMT145	AGGCAAGCTTTATTGAGGCTTAAGCAG
SIVcpzBF1167	AGGCAAGCTTTATTGAGCGTTAAGCAG
PCR primers	
SIVcpzMB897	Gag-F: ATGGGTGCGAGAGCGTCAGTATTAACGGGAG
	Gag-R: CTATTCTTGCTGCGACAACGGGTCGTTGCCA
SIVcpzBF1167	Gag-F: ATGGGTGCGAGAGCGTCAGTATTGAGGGGAG
	Gag-R: TCATTGGTCGCTGCCAAAGATGGATTTCAGG
SIVcpzMB897	Pol-F: TTTTTTAGGGAAAATCTGGCCTCCCCGCAA
	Pol-R: TTAACTCTCATCCTGTCTATCTGCCAGACAATCATTACC
SIVcpzBF1167	Pol-F: TTTTTTAGGGAAACGCACCCCCTGGTGGG
	Pol-R: CTAATCCTCATTCTGTCTATCTGCCACACCACCCGCAC
SIVcpzMB897	Env-F: ATGAAAGTGATGGGGACACAGAGGAGTTGGAAGC
	Env-R: TTATAGCAAAGCTCTTTCTAAACCTTGTCTAATTCTTCTAG
SIVcpzBF1167	Env-F: ATGAAAATGGCCTTATTAATTGGATGGATCCTGAC
	Env-R: TTAGTTTAGAGCAATTTCTAATCCCTGCCTGATTCTAGTTG
SIVcpzMB897	Vpu-F: ATGGAAATATTCATAATCTT
	Vpu-R: CTAATAACCCCTAATAGC
SIVcpzEK505	Vpu-F: ATGTTGTTGCTTATAAAG
	Vpu-R: TCAGACCCAATTATCTT
SIVcpzMT145	Vpu-F: ATGCAGCTAGAAATTG
	Vpu-R: TCACCAAAACAGGAT
SIVcpzBF1167	Vpu-F: CTGTGGCAATTTTTACA
	Vpu-R: TTACAACAGAAAATAATTGT

[a] F, forward; R, reverse; P, probe.

and P. The coordinates of *pol* gene are 3887 to 4778 on the HIV-1/HXB2 genome. The *pol* sequences were aligned using MUSCLE 3.8 to generate multiple-sequence alignment in the PHYLIP interleaved format (21). The alignment used maximum iteration to get the highest accuracy. Phylogenetic analysis was performed using PHYML 3.0 (22), an implementation of the maximum likelihood method. The tree was visualized by FigTree 1.4.2 (23). The sequences of *env*, *gag*, and *pol* genes from hu-BLT-mouse samples were processed using an in-house-developed pipeline to identify the mutation sites that had a >5% mutation rate in order to reduce background noise. To exclude random mutations, we used the following criteria to identify significant mutations. The nucleotide changes are nonsynonymous, which resulted in the same amino acid change in all sequenced animals of each group. Meanwhile, the average nucleotide substitution must be above 20%. The identified nucleotide changes were converted into amino acid mutations. The corresponding positions for these mutations were mapped to and annotated on HIV-1 GP160 trimer using UCSC Chimera 1.10.2 (23). The file for PDB 3J5M for the trimer structure was downloaded from the RCSB Protein Data Bank. The sequence logos for these identified Env AA mutations were generated from 55 HIV-1 M group and 23 available SIVcpz sequences using WebLogo 2.8.2 (http://weblogo.berkeley.edu) (24).

Statistics. The log rank and Gehan-Breslow-Wilcoxon tests (25) were used to determine the statistical significance of the Kaplan-Meier plots for conversion to infected status between SIVcpz and HIV-1_{SUMA} groups and between different SIVcpz groups. Two-way analysis of variance (ANOVA) was used to test the statistical difference of pVL of SIVcpz and HIV-1_{SUMA} at different time points postinoculation. Both tests were performed by using Graphpad Prism software (Graphpad; San Diego, CA, USA). *P* values of <0.05 were considered significant.

Accession number(s). All sequencing data have been submitted to NCBI BioSample database under the accession numbers SAMN04569153 to SAMN04569164.

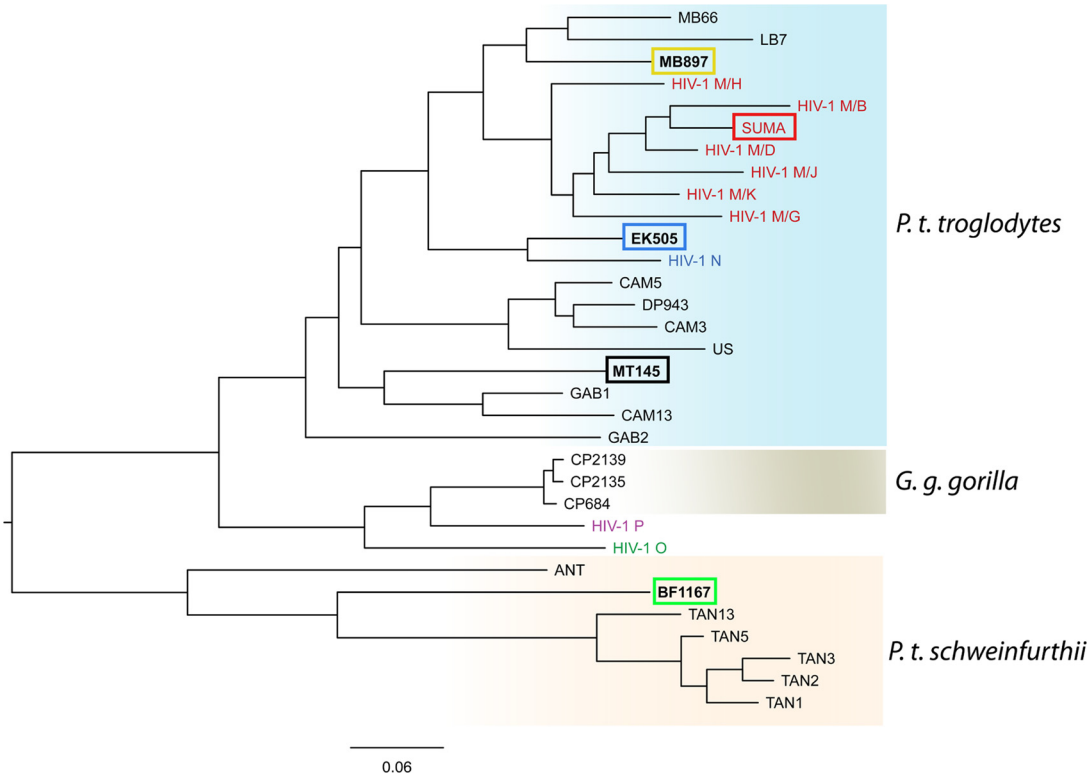

FIG 1 The phylogeny of SIVcpz, SIVgor, and HIV-1. The evolutionary relationship of SIVcpz, SIVgor, and HIV-1 groups M, N, O, and P is based on *pol* sequences, whose coordinates are 3887 to 4778 on the HIV-1/HXB2 genome. The viruses used in this study are highlighted in boxes, and virus host species are indicated on the right. The scale bar represents 0.06 amino acid replacements per site. *G. g. gorilla*, *Gorilla gorilla* subsp. *gorilla*.

RESULTS AND DISCUSSION

Four SIVcpz strains infect hu-BLT mice. We first tested whether divergent strains of SIVcpz can infect hu-BLT mice. We selected 4 phylogenetically divergent SIVcpz strains to represent the inferred ancestral viruses of pandemic HIV-1 group M (SIVcpzMB897) and nonpandemic HIV-1 group N (SIVcpzEK505) (6, 26), as well as SIVcpzMT145 (6) and SIVcpzBF1167 (27), whose viral lineages have not been found in humans (4, 8). We included HIV-1_{SUMA}, a

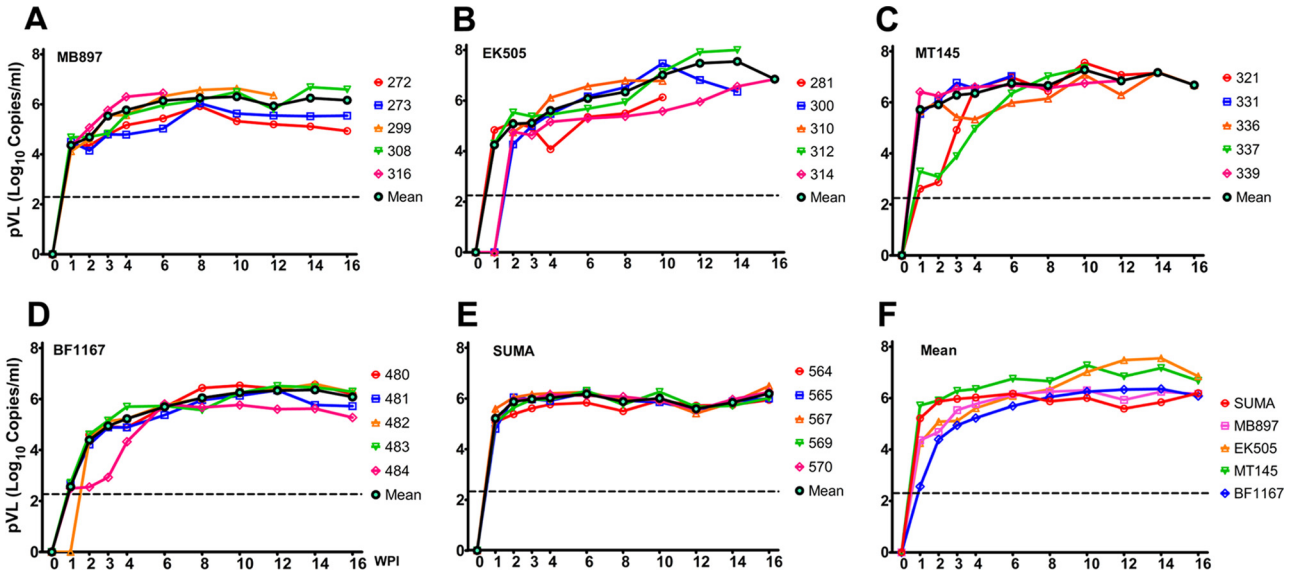

FIG 2 SIVcpz pVL kinetics. (A to E) Plasma VL over the course of up to 16 wpi in 5 groups of hu-BLT mice inoculated with a high dose of each virus: SIVcpzMB897 (A), SIVcpzEK505 (B), SIVcpzMT145 (C), SIVcpzBF1167 (D), and HIV-1_{SUMA} (E). (F) Plasma VL kinetics of all 5 groups based on the mean values. The dashed line indicates the detection limit of pVL.

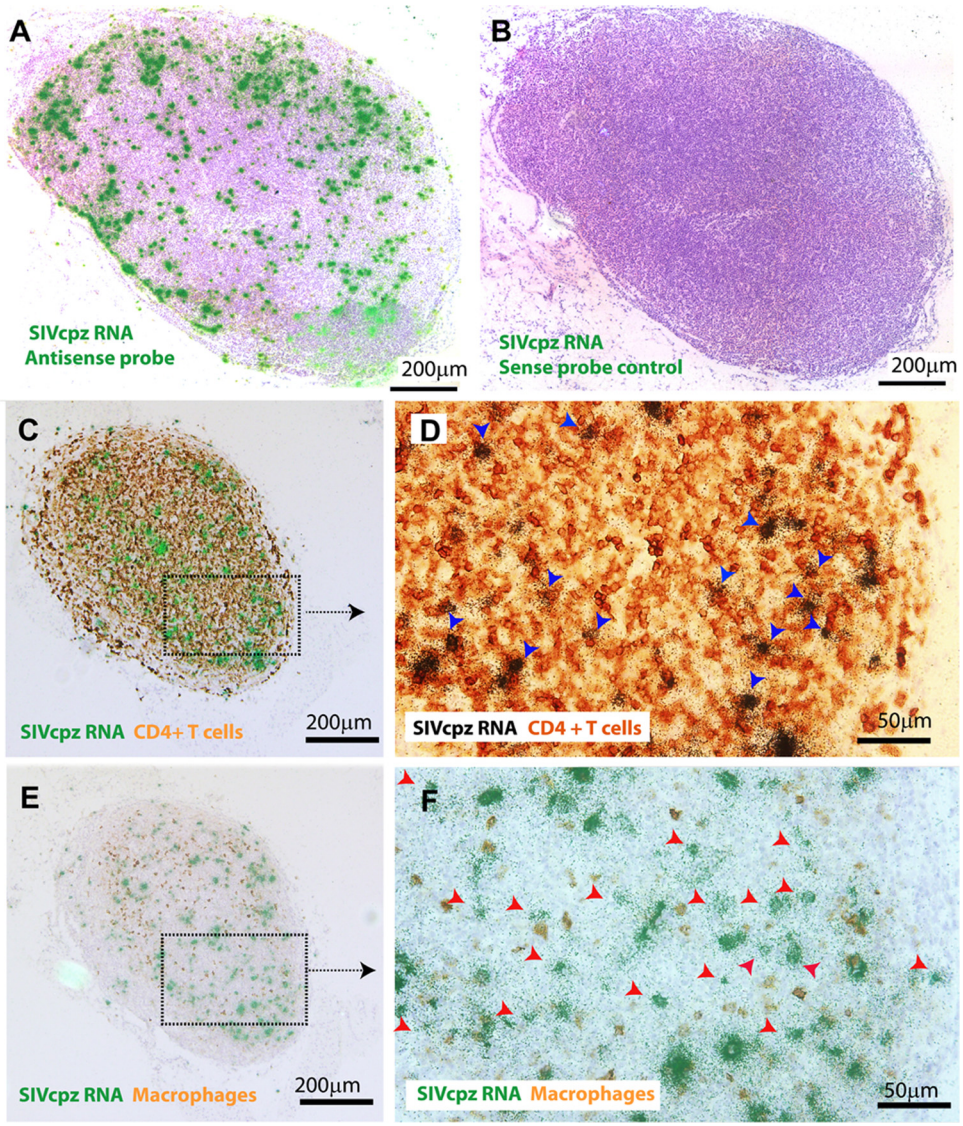

FIG 3 SIVcpz RNA$^+$ cells and infected cell types in lymphoid tissues. Representative images of lymph node tissues of hu-BLT mice at 16 wpi detected using *in situ* hybridization (ISH) with ^{35}S-labeled probes (A and B) and a combination of ISH and IHC staining (C to F). Viral RNA$^+$ cells in SIVcpzEK505-infected hu-BLT mouse detected with antisense probe (A) or with sense probe as a negative control (B). The majority of viral RNA$^+$ cells are colocalized with CD4$^+$ T cells (C and D, blue arrows), and some of the viral RNA$^+$ cells are colocalized with macrophages (E and F) in SIVcpzBF1167-infected hu-BLT mouse. Viral RNA$^+$ cells that are not colocalized with macrophages are indicated with red arrows (F).

clade B founder virus derived from an individual acutely infected with HIV-1 (28), representing the pandemic HIV-1 group M (HIV-1/M). Hu-BLT mice with high human immune reconstitution were randomly divided into 5 groups ($n = 5$/group) (Table 1), from which each hu-BLT mouse was inoculated intraperitoneally (i.p.) with the dosage of $3 \times 10^4 \pm 0.2 \times 10^4$ infectious units/mouse (IU). It has been reported that the simian-to-human cross-species transmissions of SIVcpz in Africa occurred mainly through human contact with infected chimpanzee blood through events such as hunting, bush meat preparation, and bites from infected apes (4, 8, 9); thus, we did not inoculate virus through a mucosal route. Peripheral blood was collected weekly in the first 4 weeks postinoculation (wpi) and once every 2 weeks thereafter for a total of 16 weeks. Plasma viral loads (pVL) were quantified using qRT-PCR with strain-specific primers and probes (Table 2). As expected, pVL in HIV-1_{SUMA}-infected mice reached a plateau ($\sim 10^6$ copies/ml) from 2 to 16 wpi (Fig. 2E). Strikingly, all four SIVcpz strains can infect and replicate in hu-BLT mice with kinetics similar to that of HIV-1, regardless of whether they come from *P. troglodytes* subsp. *troglodytes* or *P. troglodytes* subsp. *schweinfurthii*, including SIVcpzBF1167 and SIVcpzMT145, whose viral lineages have not been found in humans (Fig. 2A to D). Of note, the timing of reaching the pVL plateau for SIVcpzBF1167 was delayed compared to HIV-1_{SUMA} ($P < 0.01$ at 2 wpi; $P < 0.001$ at 3, 4, 6 wpi) (Fig. 2F).

Lymph node tissues were collected after euthanasia at 16 wpi. Using *in situ* hybridization (ISH) with ^{35}S-labeled strain specific antisense probes, we detected viral RNA$^+$ cells in these tissues from all hu-BLT mice that were infected with each different SIVcpz strain (Fig. 3A; one SIVcpzEK505-infected animal is shown as a

TABLE 3 SIVcpz-infected cell types

SIVcpz	% Colocalization of vRNA and:	
	$CD4^+$ cells	Macrophages
MB897	88.95	14.29
EK505	89.29	10.07
MT145	90.37	13.85
BF1167	85.96	13.3
Mean ± SD	88.64 ± 1.89	12.88 ± 1.91

representative) compared with the negative control using sense probes (Fig. 3B). We found that humanized mice are susceptible to all 4 divergent strains of SIVcpz infection *in vivo*, suggesting that SIVcpz strains that have not been found in humans have the ability to infect human cells, which may generate an HIV-1-like zoonosis. SIVcpz-infected cell types *in vivo* were determined by using a combination of ISH and immunohistochemical (IHC) staining, and we demonstrated that the majority of detectable SIVcpz infection occurs in $CD4^+$ T cells for all studied SIVcpz strains (88.64% ± 1.89%) (Table 3; Fig. 3C and D, blue arrows; an SIVcpzBF1167-infected animal is used as a representative), and some of the detectable SIVcpz infection occurs in macrophages (12.88% ± 1.91%) (Table 3; Fig. 3E and F). The infected cell types are similar among 4 strains of SIVcpz-infected hu-BLT mice, which is consistent with HIV-1 infection in humans (20).

Cross-species transmissibility of 4 divergent strains of SIVcpz viruses to humans. Because SIVcpzMT145 (*P. troglodytes* subsp. *troglodytes*) and SIVcpzBF1167 (*P. troglodytes* subsp. *schweinfurthii*) inferred descendant viruses have not been found in humans, our hypothesis is that different SIVcpz strains have diverse cross-species transmissibility to infect humans. We first sought to normalize the inoculum of the 4 SIVcpz strains and HIV-1_{SUMA}. Since a dose based on infectious units or 50% tissue culture infective dose ($TCID_{50}$) may be biased due to the human-origin indicator cells, we used reverse transcriptase activity to normalize the dose of inoculum (19). We then reduced the inoculation dose to 0.52 RT units, which is significantly lower (9.42-fold reduction of IU on average) than the high-dose inoculum that we used in initial infections of hu-BLT mice. We inoculated hu-BLT mice with a repeated, low dose of SIVcpz through the i.p. route. hu-BLT mice were divided into 5 groups ($n = 5$ or 6 for each group) (Table 1), from which each mouse was inoculated with each respective virus strain. Plasma VL was measured at 2 and 4 wpi to determine the infection status. If pVL was negative at 4 wpi, the animal was considered uninfected and reinoculated, which was followed by pVL measurement until all animals were demonstrably infected. The Kaplan-Meier plots for conversion to infected status for each SIVcpz group were compared to that of the HIV-1_{SUMA} group to quantify the barrier of cross-species transmission for each strain. There are significant differences in the number of inoculations needed for infection between SIVcpzMT145 (Fig. 4C) and SIVcpzBF1167 (Fig. 4D) compared with HIV-1_{SUMA} ($P = 0.0495$ and $P = 0.0027$, respectively). Although differences are not significant, SIVcpzMB897 (Fig. 4A) and SIVcpzEK505 (Fig. 4B) required a higher number of inoculations than HIV-1_{SUMA} to infect all of the hu-BLT mice ($P = 0.3613$ and $P = 0.3173$, respectively). We then tested the differences between SIVcpz strains in the number of inoculations needed for infection. There are significant differences between SIVcpzMB897 and SIVcpzBF1167 ($P = 0.0076$) as well as between SIVcpzEK505 and SIVcpzBF1167 ($P = 0.0131$); however, there are no significant

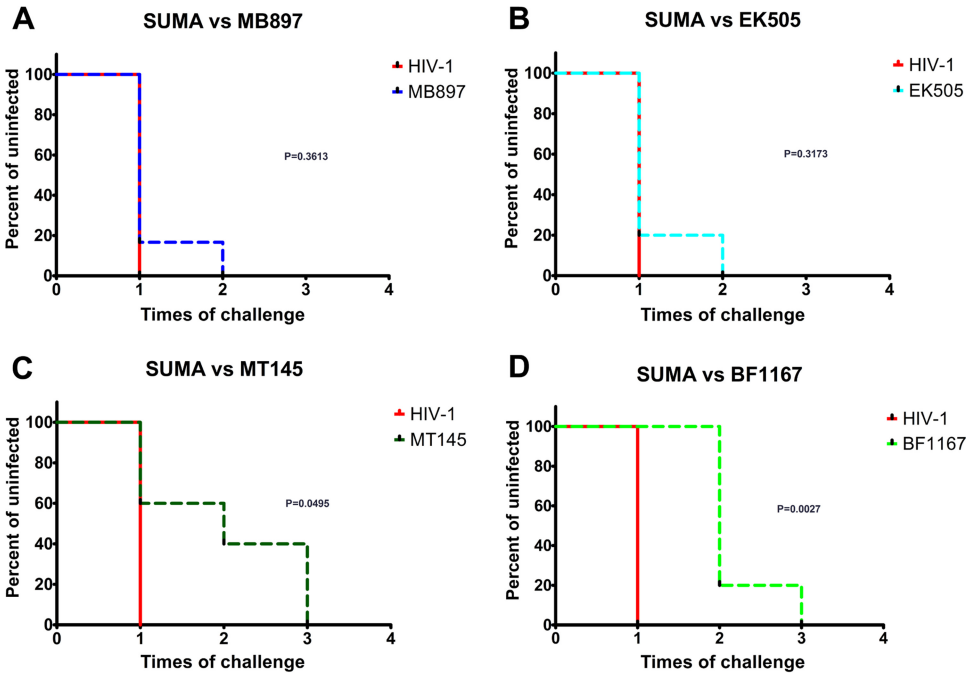

FIG 4 Cross-species transmission barrier of SIVcpz. Five groups of hu-BLT mice were inoculated with a low dose of SIVcpz or HIV-1_{SUMA} normalized through RT activity ($n = 5$ or 6). The Kaplan-Meier plots for conversion to infected status are in red for HIV-1_{SUMA} (A through D), in dark blue for SIVcpzMB897 (A), in light blue for SIVcpzEK505 (B), in dark green for SIVcpzMT145 (C), and in light green for SIVcpzBF1167 (D). The *P* value indicates the significance of differences between the two curves, and *P* values of <0.05 are considered significant.

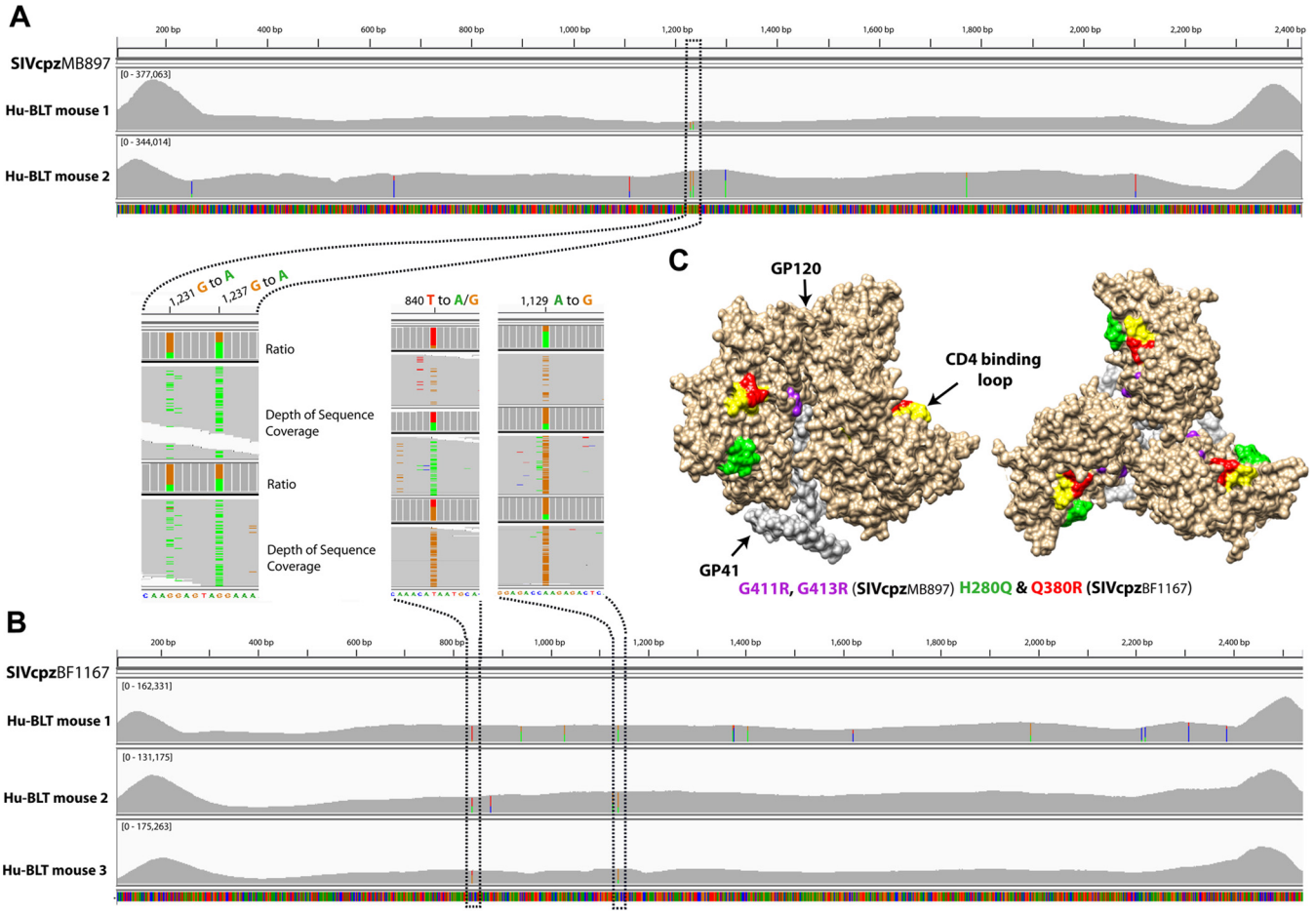

FIG 5 Env sequencing revealed the mutation of SIVcpz *in vivo* at 14 wpi. The coverage and depth (square brackets) of next-generation sequencing of SIVcpzMB897 and SIVcpzBF1167 are shown. The expanded images highlight the mutation positions and ratios: A is in green, T in red, G in orange, and C in blue. (A) SIVcpzMB897 cross-animal mutations at positions 1231 and 1237 in hu-BLT mice 273 and 308. (B) SIVcpzBF1167 cross-animal mutations at positions 840 and 1129 in hu-BLT mice 480, 482, and 483. (C) Amino acid mutations mapped to the corresponding positions on HIV-1 Env trimer. GP120 is in light brown, GP41 is in light gray, the CD4 binding loop is in yellow, SIVcpzMB897 G411R and G413R are in purple, SIVcpzBF1167 H280Q is in green, and Q380R is in red.

differences between SIVcpzMB897 and SIVcpzEK505 ($P = 0.9818$) or between SIVcpzMT145 and SIVcpzBF1167 ($P = 0.7317$). Thus, the cross-species transmission barriers of different SIVcpz strains are correlated with their phylogenetic distance to HIV-1/M (Fig. 1). Our study revealed that the different cross-species transmission barriers of SIVcpz play an important role in determining the establishment and spatial dissemination of pandemic HIV-1. It is also plausible that the different cross-species transmission barriers of SIVcpz may have also impacted the efficiency of initial human-to-human transmission.

Mutations of SIVcpz *in vivo*. It has been proposed that viral adaptation was required to overcome host-specific innate restriction factors found between chimpanzees and humans (29–32). To assess the *in vivo* mutations of SIVcpz, we sequenced the major viral genes (*gag*, *pol*, and *env*) of SIVcpzMB897 and SIVcpzBF1167 in hu-BLT mice at 14 wpi. The following criteria were used to identify each significant mutation: nucleotide changes had to be nonsynonymous, resulting in the same amino acid change for all sequenced animals, and the average nucleotide substitution rate from all sequenced animals had to be >20%. We did not find any cross-animal mutation in *gag* or *pol* that accumulated more than 10% on average at 14 wpi compared with the inoculum. However, as shown in Fig. 5A, next-generation sequencing (NGS) of SIVcpzMB897*env* gene revealed a consistent G-to-A change at positions 1231 (24.45% on average) and 1237 (53.53% on average) in two sequenced animals compared with sequences in the inoculum. The detected nucleotide changes correspond to G411R and G413R, respectively. As shown in Fig. 5B, NGS of SIVcpzBF1167 *env* gene revealed a consistent T-to-A/G change (A/G is synonymous) at position 840 (41.20% on average) and an A-to-G change at position 1129 (58.23% on average) in all three sequenced animals. The detected nucleotide changes correspond to H280Q and Q380R, respectively. We also checked whether the observed SIVcpz mutations exist in HIV-1 Env, as shown in the mutation sequence logos (Fig. 6), and we found that all the mutated amino acids exist in HIV-1 but three of them are absent in SIVcpz (SIVcpz BF1167 H280Q and Q380R and MB897 G413R). For the SIVcpz BF1167 H280Q mutation, Q is absent in SIVcpz but present in HIV-1 with low frequency. Similarly, for the mutation Q380R, R is absent in SIVcpz but present in HIV-1 with low frequency. For the MB897 G411R mutation, R is present in

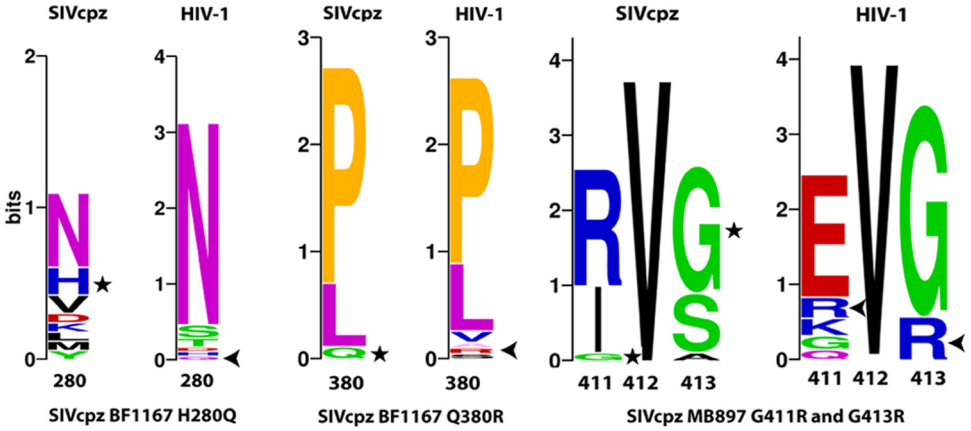

FIG 6 Sequence logos for the identified Env AA mutations. For the SIVcpz BF1167 H280Q mutation, Q is absent in SIVcpz but present in HIV-1 with low frequency; similarly, for mutation Q380R, R is absent in SIVcpz but present in HIV-1 with low frequency. For the MB897 G411R mutation, R is present in both SIVcpz and HIV-1; and for the MB897 G413R mutation, R is absent in SIVcpz but present in HIV-1. Star, original AA in the SIVcpz viruses; arrow, mutated AA in HIV-1 at their corresponding positions.

both SIVcpz and HIV-1; for the MB897 G413R mutation, R is absent in SIVcpz but present in HIV-1.

Since SIVcpz Env three-dimensional (3D) structures are not available, the locations of these mutations were mapped to the corresponding position on the HIV-1 gp160 trimer (Fig. 5C). The G411R, G413R, H280Q, and Q380R mutations were located at the interface between gp41 and gp120, adjacent to or within the CD4 binding loop, respectively (Fig. 5C). The CD4 binding loop of HIV-1 gp120 is essential for interacting with the primary CD4 receptor during viral entry and a site of vulnerability for broadly neutralizing antibodies to target (33, 34).

Previously, it was reported that all known strains of SIVcpz at position Gag 30 encode a Met (M) or Leu, but many current pandemic HIV-1 strains encode Arg (R) or Lys at that position (35, 36). Moreover, SIVcpz Gag M30R has a fitness advantage over its wild-type counterpart as observed in a replication competition assay using human cells and tonsillar explant cultures (35, 36). Thus, we compared the fitness of Gag M30R mutants

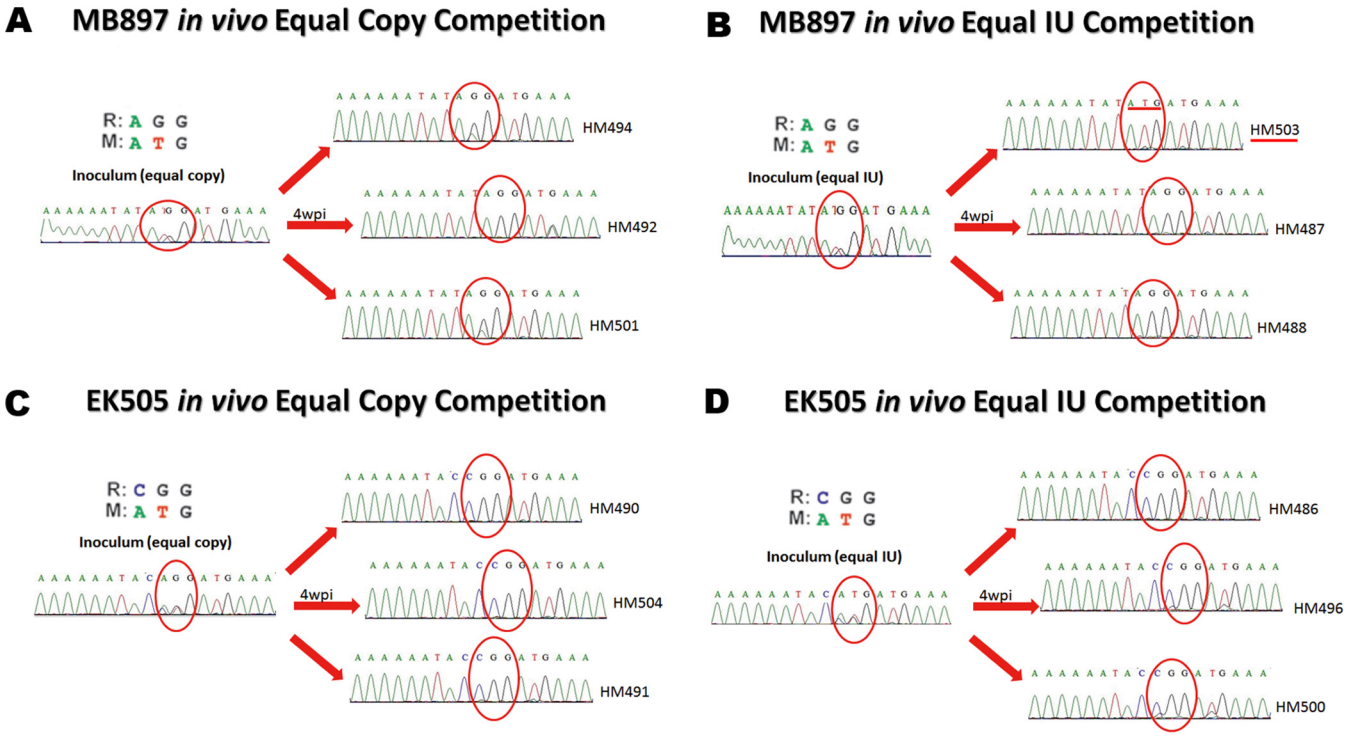

FIG 7 Gag M30R mutant and wild-type *in vivo* competition at 4 wpi. Red circle, position of Gag 30. (A) SIVcpzMB897 *in vivo* equal-copy-number competition. (B) SIVcpzMB897 *in vivo* equal-IU competition. The red line highlights the only animal with opposite selection. (C) SIVcpzEK505 *in vivo* equal-copy-number competition. (D) SIVcpzEK505 *in vivo* equal-IU competition.

of SIVcpzMB897 and SIVcpzEK505 to the fitness of their wild-type counterparts in an *in vivo* competition study. To eliminate the possibility that an equal copy number may have unequal infectious units, an equal-infectious-units (IU) mixture competition was also conducted; this was not done in previously reported explant tonsil culture studies. Four groups of hu-BLT mice (n = 3/group) were used (Table 1), and each mouse was inoculated with an equal-copy-number or equal-IU mix of wild-type and mutant virus. At 4 wpi, the SIVcpzMB897 M30R mutant virus was dominant in 5 (3 in the equal-copy-number group and 2 in the equal-IU group) of 6 animals (Fig. 7A and B). Interestingly, one animal showed the opposite selection (wild-type dominant) after 4 weeks of competition (Fig. 7B). The SIVcpzEK505 M30R mutant was dominant in all 6 mice (Fig. 7C and D). From these *in vivo* competition assays, we conclude that the GagM30R mutation confers a fitness advantage over its wild-type counterpart in most cases. However, we did not detect this Gag M30R mutation after 14 weeks of infection in the hu-BLT mice; one plausible explanation is that this *de novo* adaptation may need more time.

A previous report showed that the *vpu* is also important in the evolution of SIVcpz to HIV-1 to antagonize tetherin function (31). Thus, we also sequenced the full-length *vpu* gene of 4 SIVcpz strain-infected hu-BLT mice (n = 3/group) at 14 wpi using bulk sequencing. The *vpu* sequences of all 12 samples at 14 wpi are identical to the inoculum sequences, which may indicate that the *de novo* generation of this adaptation of *vpu* may also need additional time or the selective pressure that would have led to those substitutions may not be present in hu-BLT mice.

In short, using the hu-BLT mouse model, our results for the first time clearly demonstrate that hu-BLT mice are susceptible to all studied SIVcpz strains *in vivo*, including the inferred ancestral viruses of pandemic and nonpandemic HIV-1 groups M (SIVcpzMB897) and N (SIVcpzEK505), as well as the strains that have not been found in humans (SIVcpzMT145 and SIVcpzBF1167). Importantly, the transmissibility of different SIVcpz strains crossing the interspecies barrier to infect humanized mice is inversely correlated with their phylogenetic distance to pandemic HIV-1. We also identified *in vivo* mutations of SIVcpzMB897 (Env G411R and G413R) and SIVcpzBF1167 (Env H280Q and Q380R) at 14 weeks postinoculation. Together, our results recapitulated the events of SIVcpz cross-species transmission to humans and identified *in vivo* mutations that occurred in the first 16 weeks of infection, providing *in vivo* experimental evidence that the origins of HIV-1 are the consequence of SIVcpz crossing over to humans. This study also revealed that SIVcpz viruses whose lineages have not been found in humans, although they have lower cross-species transmissibility, still have the potential to cause an HIV-1-like zoonosis. Since wild NHPs, especially our closest relatives, the great apes, still harbor many SIV strains, these reservoirs may continue to pose a risk for potential zoonotic outbreak in humans.

ACKNOWLEDGMENTS

We thank Lance Daharsh, Charles Wood, and John West for their critical reading of the manuscript.

Q.L. and Z.Y. conceived the idea and with B.K. designed the experiments; B.K. provided the virus plasmids; Z.Y., B.K., and C.F. prepared the viral stocks; G.K., W.L., Z.Y., and W.F. conducted animal infection and tissue dissection; Z.Y. prepared the *in situ* probes; G.K. conducted the ISH and IHC staining; F.M. and Z.Y. did the bioinformatics analysis; Z.Y. did all other experiments; Z.Y. and Q.L. wrote the manuscript.

This project has been funded in part with NIH P30GM103509, NIH R01 DK087625 (Q.L.), and the Start-up funds from the University of Nebraska—Lincoln (Q.L.), with the National Cancer Institute, National Institutes of Health, under Contract No. HHSN261200800001E (B.K.).

FUNDING INFORMATION

This work, including the efforts of Brandon F. Keele, was funded by HHS | NIH | National Cancer Institute (NCI) (HHSN261200800001E). This work, including the efforts of Qingsheng Li, was funded by HHS | National Institutes of Health (NIH) (P30GM103509). This work, including the efforts of Qingsheng Li, was funded by HHS | National Institutes of Health (NIH) (R01 DK087625).

REFERENCES

1. **Fauci AS, Folkers GK, Dieffenbach CW.** 2013. HIV-AIDS: much accomplished, much to do. Nat Immunol **14:**1104–1107. http://dx.doi.org/10.1038/ni.2735.
2. **Faria NR, Rambaut A, Suchard MA, Baele G, Bedford T, Ward MJ, Tatem AJ, Sousa JD, Arinaminpathy N, Pépin J, Posada D, Peeters M, Pybus OG, Lemey P.** 2014. The early spread and epidemic ignition of HIV-1 in human populations. Science **346:**56–61. http://dx.doi.org/10.1126/science.1256739.
3. **Paraskevis D, Lemey P, Salemi M, Suchard M, Van De Peer Y, Vandamme AM.** 2003. Analysis of the evolutionary relationships of HIV-1 and SIVcpz sequences using bayesian inference: implications for the origin of HIV-1. Mol Biol Evol **20:**1986–1996. http://dx.doi.org/10.1093/molbev/msg207.
4. **Sharp PM, Hahn BH.** 2011. Origins of HIV and the AIDS pandemic. Cold Spring Harb Perspect Med **1**(1):a006841. http://dx.doi.org/10.1101/cshperspect.a006841.
5. **Huet T, Cheynier R, Meyerhans A, Roelants G, Wain-Hobson S.** 1990. Genetic organization of a chimpanzee lentivirus related to HIV-1. Nature **345:**356–359. http://dx.doi.org/10.1038/345356a0.
6. **Keele BF, Van Heuverswyn F, Li Y, Bailes E, Takehisa J, Santiago ML, Bibollet-Ruche F, Chen Y, Wain LV, Liegeois F, Loul S, Ngole EM, Bienvenue Y, Delaporte E, Brookfield JFY, Sharp PM, Shaw GM, Peeters M, Hahn BH.** 2006. Chimpanzee reservoirs of pandemic and nonpandemic HIV-1. Science **313:**523–526. http://dx.doi.org/10.1126/science.1126531.
7. **Gao F, Bailes E, Robertson DL, Chen Y, Rodenburg CM, Michael SF, Cummins LB, Arthur LO, Peeters M, Shaw GM, Sharp PM, Hahn BH.** 1999. Origin of HIV-1 in the chimpanzee Pan troglodytes troglodytes. Nature **397:**436–441. http://dx.doi.org/10.1038/17130.
8. **Hahn BH, Shaw GM, De Cock KM, Sharp PM.** 2000. AIDS as a zoonosis: scientific and public health implications. Science **287:**607–614. http://dx.doi.org/10.1126/science.287.5453.607.
9. **Mourez T, Simon F, Plantier J-C.** 2013. Non-M variants of human immunodeficiency virus type 1. Clin Microbiol Rev **26:**448–461. http://dx.doi.org/10.1128/CMR.00012-13.
10. **Santiago ML, Rodenburg CM, Kamenya S, Bibollet-Ruche F, Gao F, Bailes E, Meleth S, Soong SJ, Kilby JM, Moldoveanu Z, Fahey B, Muller MN, Ayouba A, Nerrienet E, McClure HM, Heeney JL, Pusey AE, Collins DA, Boesch C, Wrangham RW, Goodall J, Sharp PM, Shaw GM, Hahn BH.** 2002. SIVcpz in wild chimpanzees. Science **295:**465. http://dx.doi.org/10.1126/science.295.5554.465.
11. **Worobey M, Santiago ML, Keele BF, Ndjango J-BN, Joy JB, Labama BL, Dhed'a BD, Rambaut A, Sharp PM, Shaw GM, Hahn BH.** 2004. Origin of AIDS: contaminated polio vaccine theory refuted. Nature **428:**820–820. http://dx.doi.org/10.1038/428820a.
12. **Sharp PM, Shaw GM, Hahn BH.** 2005. Simian immunodeficiency virus infection of chimpanzees. J Virol **79:**3891–3902. http://dx.doi.org/10.1128/JVI.79.7.3891-3902.2005.
13. **Peeters M, Honore C, Huet T, Bedjabaga L, Ossari S, Bussi P, Cooper RW, Delaporte E.** 1989. Isolation and partial characterization of an HIV-related virus occurring naturally in chimpanzees in Gabon. AIDS **3:**625–630. http://dx.doi.org/10.1097/00002030-198910000-00001.
14. **Shultz LD, Brehm MA, Garcia-Martinez JV, Greiner DL.** 2012. Humanized mice for immune system investigation: progress, promise and challenges. Nat Rev Immunol **12:**786–798. http://dx.doi.org/10.1038/nri3311.
15. **Melkus MW, Estes JD, Padgett-Thomas A, Gatlin J, Denton PW, Othieno FA, Wege AK, Haase AT, Garcia JV.** 2006. Humanized mice

mount specific adaptive and innate immune responses to EBV and TSST-1. Nat Med **12:**1316–1322. http://dx.doi.org/10.1038/nm1431.
16. **VandeWoude S, Apetrei C.** 2006. Going wild: lessons from naturally occurring T-lymphotropic lentiviruses. Clin Microbiol Rev **19:**728–762. http://dx.doi.org/10.1128/CMR.00009-06.
17. **Wang L-X, Kang G, Kumar P, Lu W, Li Y, Zhou Y, Li Q, Wood C.** 2014. Humanized-BLT mouse model of Kaposi's sarcoma-associated herpesvirus infection. Proc Natl Acad Sci U S A **111:**3146–3151. http://dx.doi.org/10.1073/pnas.1318175111.
18. **Li Q, Tso FY, Kang G, Lu W, Li Y, Fan W, Yuan Z, Destache CJ, Wood C.** 2015. Early initiation of antiretroviral therapy can functionally control productive HIV-1 infection in humanized-BLT mice. J Acquir Immune Defic Syndr **69:**519–527. http://dx.doi.org/10.1097/QAI.0000000000000687.
19. **Marozsan AJ, Fraundorf E, Abraha A, Baird H, Moore D, Troyer R, Nankja I, Arts EJ.** 2004. Relationships between infectious titer, capsid protein levels, and reverse transcriptase activities of diverse human immunodeficiency virus type 1 isolates. J Virol **78:**11130–11141. http://dx.doi.org/10.1128/JVI.78.20.11130-11141.2004.
20. **Li Q, Duan L, Estes JD, Ma Z-M, Rourke T, Wang Y, Reilly C, Carlis J, Miller CJ, Haase AT.** 2005. Peak SIV replication in resting memory CD4+ T cells depletes gut lamina propria CD4+ T cells. Nature **434:**1148–1152.
21. **Edgar RC.** 2004. MUSCLE: multiple sequence alignment with high accuracy and high throughput. Nucleic Acids Res **32:**1792–1797. http://dx.doi.org/10.1093/nar/gkh340.
22. **Guindon S, Dufayard JF, Lefort V, Anisimova M, Hordijk W, Gascuel O.** 2010. New algorithms and methods to estimate maximum-likelihood phylogenies: assessing the performance of PhyML 3.0. Syst Biol **59:**307–321. http://dx.doi.org/10.1093/sysbio/syq010.
23. **Pettersen EF, Goddard TD, Huang CC, Couch GS, Greenblatt DM, Meng EC, Ferrin TE.** 2004. UCSF Chimera—a visualization system for exploratory research and analysis. J Comput Chem **25:**1605–1612. http://dx.doi.org/10.1002/jcc.20084.
24. **Crooks GE, Hon G, Chandonia JM, Brenner SE.** 2004. WebLogo: a sequence logo generator. Genome Res **14:**1188–1190. http://dx.doi.org/10.1101/gr.849004.
25. **Le CT.** 1997. Applied survival analysis. John Wiley and Sons, New York, NY.
26. **Heuverswyn FV, Li Y, Bailes E, Neel C, Lafay B, Keele BF, Shaw KS, Takehisa J, Kraus MH, Loul S, Butel C, Liegeois F, Yangda B, Sharp PM, Mpoudi-Ngole E, Delaporte E, Hahn BH, Peeters M.** 2007. Genetic diversity and phylogeographic clustering of SIVcpzPtt in wild chimpanzees in Cameroon. Virology **368:**155–171. http://dx.doi.org/10.1016/j.virol.2007.06.018.
27. **Li Y, Ndjango J-B, Learn GH, Ramirez MA, Keele BF, Bibollet-Ruche F, Liu W, Easlick JL, Decker JM, Rudicell RS, Inogwabini B-I, Ahuka-Mundeke S, Leendertz FH, Reynolds V, Muller MN, Chancellor RL, Rundus AS, Simmons N, Worobey M, Shaw GM, Peeters M, Sharp PM, Hahn BH.** 2012. Eastern chimpanzees, but not bonobos, represent a simian immunodeficiency virus reservoir. J Virol **86:**10776–10791. http://dx.doi.org/10.1128/JVI.01498-12.
28. **Ochsenbauer C, Edmonds TG, Ding H, Keele BF, Decker J, Salazar MG, Salazar-Gonzalez JF, Shattock R, Haynes BF, Shaw GM, Hahn BH, Kappes JC.** 2012. Generation of transmitted/founder HIV-1 infectious molecular clones and characterization of their replication capacity in CD4 T lymphocytes and monocyte-derived macrophages. J Virol **86:**2715–2728. http://dx.doi.org/10.1128/JVI.06157-11.
29. **Sauter D, Schindler M, Specht A, Landford WN, Münch J, Kim K-A, Votteler J, Schubert U, Bibollet-Ruche F, Keele BF, Takehisa J, Ogando Y, Ochsenbauer C, Kappes JC, Ayouba A, Peeters M, Learn GH, Shaw G, Sharp PM, Bieniasz P, Hahn BH, Hatziioannou T, Kirchhoff F.** 2009. Tetherin-driven adaptation of Vpu and Nef function and the evolution of pandemic and nonpandemic HIV-1 strains. Cell Host Microbe **6:**409–421. http://dx.doi.org/10.1016/j.chom.2009.10.004.
30. **Heeney JL, Dalgleish AG, Weiss RA.** 2006. Origins of HIV and the evolution of resistance to AIDS. Science **313:**462–466. http://dx.doi.org/10.1126/science.1123016.
31. **Kirchhoff F.** 2010. Immune evasion and counteraction of restriction factors by HIV-1 and other primate lentiviruses. Cell Host Microbe **8:**55–67. http://dx.doi.org/10.1016/j.chom.2010.06.004.
32. **Duggal NK, Emerman M.** 2012. Evolutionary conflicts between viruses and restriction factors shape immunity. Nat Rev Immunol **12:**687–695. http://dx.doi.org/10.1038/nri3295.
33. **Zhou T, Xu L, Dey B, Hessell AJ, Van Ryk D, Xiang S-H, Yang X, Zhang M-Y, Zwick MB, Arthos J, Burton DR, Dimitrov DS, Sodroski J, Wyatt R, Nabel GJ, Kwong PD.** 2007. Structural definition of a conserved neutralization epitope on HIV-1 gp120. Nature **445:**732–737. http://dx.doi.org/10.1038/nature05580.
34. **Kwong PD, Mascola JR.** 2012. Human antibodies that neutralize HIV-1: identification, structures, and B cell ontogenies. Immunity **37:**412–425. http://dx.doi.org/10.1016/j.immuni.2012.08.012.
35. **Wain LV, Bailes E, Bibollet-Ruche F, Decker JM, Keele BF, Van Heuverswyn F, Li Y, Takehisa J, Ngole EM, Shaw GM, Peeters M, Hahn BH, Sharp PM.** 2007. Adaptation of HIV-1 to its human host. Mol Biol Evol **24:**1853–1860. http://dx.doi.org/10.1093/molbev/msm110.
36. **Bibollet-Ruche F, Heigele A, Keele BF, Easlick JL, Decker JM, Takehisa J, Learn G, Sharp PM, Hahn BH, Kirchhoff F.** 2012. Efficient SIVcpz replication in human lymphoid tissue requires viral matrix protein adaptation. J Clin Invest **122:**1644–1652. http://dx.doi.org/10.1172/JCI61429.